

Extreme high resolution scanning electron microscopy (XHR SEM) and beyond

Laurent Y. Roussel*^a, Debbie J. Stokes^a, Ingo Gestmann^a, Mark Darus^b and Richard J. Young^b

^aFEI Company, Building AAE, PO Box 80066, 5600 KA Eindhoven, The Netherlands

^bFEI Company, 5350 NE Dawson Creek Drive, Hillsboro, OR 97124, USA;

ABSTRACT

For decades, high resolution scanning electron microscopes (SEM) have strived to offer improved performance in the high and low energy regimes. High energies have always been attractive, because they lead to sub-nanometer resolution without complex electron optics, especially when using a scanning transmission electron microscopy (STEM) mode in the SEM. Lower energies have caught the attention of microscopists, due to their increased surface sensitivity, minimized charging effects or reduced depth of radiation damage. While going to very low beam landing energies was demonstrated more than 20 years ago, keeping a nanometric spot-size below 1 keV proved to be a technological challenge. Only a few years ago did the first commercial SEM succeed in delivering sub-nanometer resolution at 1 kV, but with some restrictions. Recently, the introduction of the extreme high resolution (XHR) SEM has demonstrated sub-nanometer resolution in the entire 1 to 30 kV range, thanks to a monochromatized Schottky electron source that reduces the effects of chromatic aberrations at lower energies. Of at least equal interest is the fact that the same XHR SEM can take advantage of its optics, modularity, platform stability and cleanliness developments to explore new avenues, such as high resolution imaging at very low beam energies or up to 30 kV STEM-in-SEM. For the first time, complementary information from the very surface and internal structure at the true nanometer level is obtained in the same SEM.

Keywords: SEM, scanning electron microscope, STEM, transmission, monochromator, low voltage, resolution

1. INTRODUCTION

The scanning electron microscope (SEM) continues to gain popularity owing to its relatively straightforward operation and data interpretation, its ability to resolve surface details at the micrometer and nanometer level and the possibility to access a continuously growing number of types of information [1]. Today, stretching the performance and versatility of SEMs has led to different categories of instruments. The analytical SEM typically offers an interesting balance between high resolution characterization and advanced analytical capabilities. The environmental SEM [2] makes it possible to manage more challenging samples, such as those prone to charging or contamination, as well as to observe or carry out dynamic *in situ* experiments in a controlled environment. The ultra-high resolution SEM focuses first on delivering outstanding resolution in the high and low kV regimes, while still allowing reasonable application flexibility and routine operation. Using refined electron optics, a fourth category showed during the last years that SEMs could characterize details well below the nanometer level at low kV [3] or high kV [4], but in most cases at the price of application flexibility and sample size.

Recently, another step was made by the introduction of a new type of SEM, the Magellan™ extreme high resolution (XHR) SEM, which demonstrates sub-nanometer resolution in both high and low kV regimes, on thin and bulk samples [5]. The introduction of specific electron optics were required to reach the low kV performance, in particular a source monochromator, named UniColore (UC), to minimize the effects of chromatic aberrations, as well as a beam deceleration mode [6] to further reduce the spot size and optimize image contrasts. The details of how XHR performance is achieved within the Magellan system is covered in a separate paper by Young et al [7]. While the unprecedented surface sensitivity at low kV provides a lot of potential, the technologies and elements combined in the Magellan to enable and support XHR performance open up new avenues, such as access to very high resolution and image quality at ultra-low landing energies and at higher kVs. This paper focuses on how the Magellan XHR SEM may be used at and beyond the mainstream low kV regime, to obtain complementary information at the nanometer level, both from the very surface of samples and from the bulk, using an integrated scanning transmission electron microscopy (STEM) mode.

*laurent.roussel@fei.com; phone +31 6 109 103 81; www.fei.com

2. HIGH RESOLUTION SEM AT LOW AND VERY LOW BEAM LANDING VOLTAGES

The attractiveness of working at low and very low beam landing voltages (LV-SEM) with the XHR SEM comes from the ability to combine two key ingredients. The first is spatial resolution: the column optics, monochromator (UC) - and if desired beam deceleration - are activated to keep the spot size as fine as possible. The second is high surface sensitivity, as the size and range of the interaction volume of electrons in the sample dramatically shrink when the primary electron beam voltage is decreased [8].

In low and very low kV operation, an extended set of optics modes and detectors is available, and presented in figure 1. Regarding the optics: the monochromator is naturally turned on to optimize chromatic aberrations. The immersion field is in general activated to ensure the best collection efficiency of secondary electrons in the through-the-lens detector (TLD), which proves of particular efficiency when the sample lies at a longer working distance or under a given tilt angle. The beam deceleration (BD) negative bias V_s is continuously adjustable between 0 and -4 kV, and serves different purposes. Together with UC, it improves the resolution when using low and very beam landing voltage [7]. By varying the bias V_s and choosing whether or not to apply the magnetic immersion field, the energy and trajectory of the electrons emitted from the sample may be varied to obtain the desired information from the sample, be it topographic contrast, materials contrast or both.

Two types of detectors are collecting the emitted electrons: the TLD, and the 'low Voltage high Contrast Detector' (vCD), positioned just below the final lens. In general, when looking for highest surface sensitivity, it is mostly the secondary electrons that are of interest, and a multi-electrode design of the TLD was developed for the Magellan to optimize top-down collection efficiency. While the TLD and the vCD both have the ability to collect backscattered electrons (BSE), their scope is somewhat different. The vCD offers very high sensitivity to low kV BSE and, depending on the beam deceleration bias and/or immersion field presence, gives access to pure materials contrast (no BD) or BSE topography contrasts (with BD). With its top-down location, the TLD in BSE mode offers excellent mass contrasts [7].

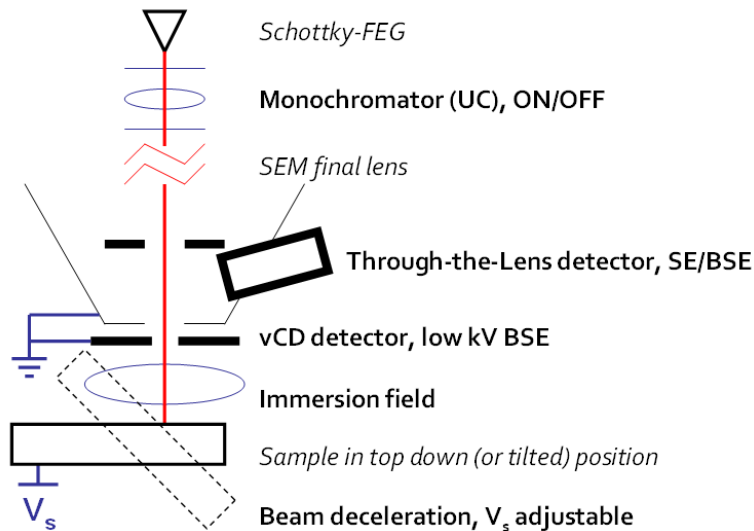


Fig. 1. Optics and detection elements of the Magellan XHR SEM for operation at low and very low kV

2.1 Imaging large samples under various incidence angles

While the value for achieving very high resolution and surface sensitivity is already high, it becomes even greater if it can be obtained on the native sample, that is, without any preparation step. First, because preparation demands time and always bears the potential risk of introducing unwanted artifacts. Further, because a sample, when rare, difficult or expensive to create, can simply not afford to be broken into pieces.

The characterization of a large wafer piece was performed to assess the XHR performance of the Magellan on large samples. The etched patterned polysilicon wafer contains typical structures that are used in the semiconductor industry for instrument calibration purposes [9]. Results are presented in figure 2.

At 2 kV, using UC but no BD (Fig. 2a), the topography on the top of the etched structures starts to become visible, but is also significantly shadowed by edge effects (but still less than if higher voltages had been used). Keeping the UC mode on and the same magnification and working distance of 1.4 mm, the acceleration voltage of the primary electron beam is decreased from 2 kV to 1.2 kV. A beam deceleration bias of -1 kV is applied to the surface of the sample, resulting in a beam landing voltage of 200 V (Fig. 2b). The edge effect is significantly reduced and the granular surface on the top of the calibration lines is clearly visible, even when viewed top-down (Fig. 2d). When tilting the same sample at 57° (fig. c), UC stays on, but tilting a large sample at a short distance creates geometry conflicts with the final lens; the working distance is therefore brought to 4.0 mm. Also the beam deceleration bias needs to be kept well below 1 kV, as the electric field between the final lens and the sample can no longer be kept uniform. A small bias of -50 V is used to boost the topographic contrast. Here also, well-defined edges and top surface details are resolved.

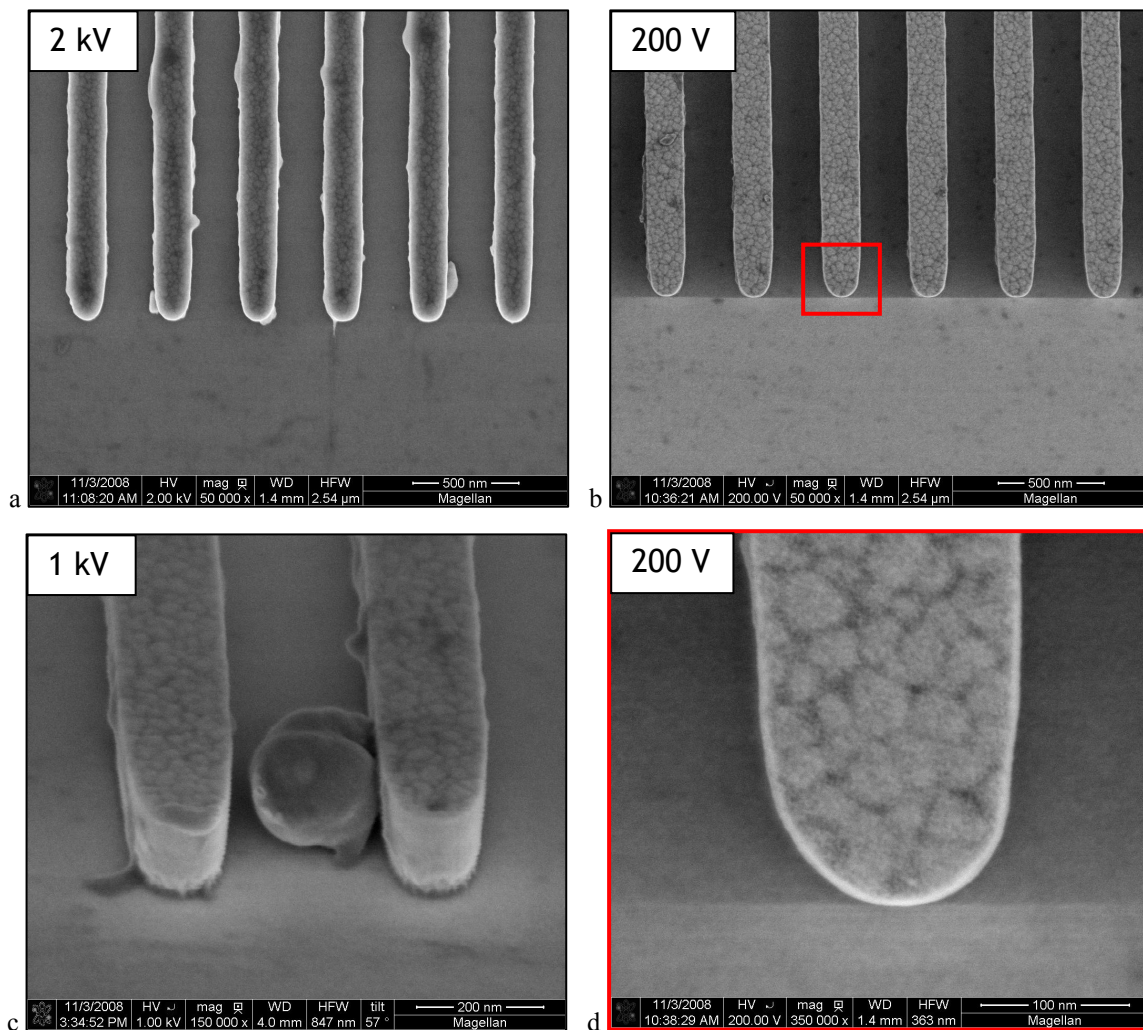


Fig. 2. Low kV characterization of a polysilicon calibration wafer piece using the TLD, under various conditions:(a) top-down, no BD and beam landing voltage of 2 kV, horizontal field width (HFW) of 2.54 μm, (b) (d) top-down, BD with $V_s=-1$ kV and beam landing voltage of 200 V, HFW of respectively 2.54 μm and 363 nm, and (c) sample tilted at 57°, BD with $V_s=-50$ V, beam landing energy of 1 kV, HFW of 847 nm.

2.2 Imaging at very low beam landing energies

At higher kVs, nanometer-scale features bound to the surface of a sample, such as tiny particles, porosities, local defects or contamination tend to vanish in the signal provided from the much larger interaction volume. Hence there is interest in going to beam landing voltages as low as 50 V to further gain in surface sensitivity, coupled with spatial resolution in the case of the XHR SEM. Another driver relates to 50 V being at around the limit where conventional contrast types known from higher beam landing voltages are balanced against new contrast mechanisms, related to the influence of the overall crystal potential, or the electronic structure of the sample [10].

A challenge in moving into the very low landing energies comes from the surface carbonaceous contamination, resulting from adsorbed hydrocarbons being decomposed under the electron beam [11]. It has been reported that as the beam landing energy goes down to about 100 eV, the spatial density of dissipated energy delivered by the incident electron beam increases [10]. As a consequence, the risk of undergoing contamination goes up. For proper imaging with electron beam voltages around 50-100 V, it is therefore essential to keep good control over both the cleanliness of the sample surface as well as the quality of the vacuum of the microscope chamber. Much effort was put in the Magellan XHR SEM to address both [7].

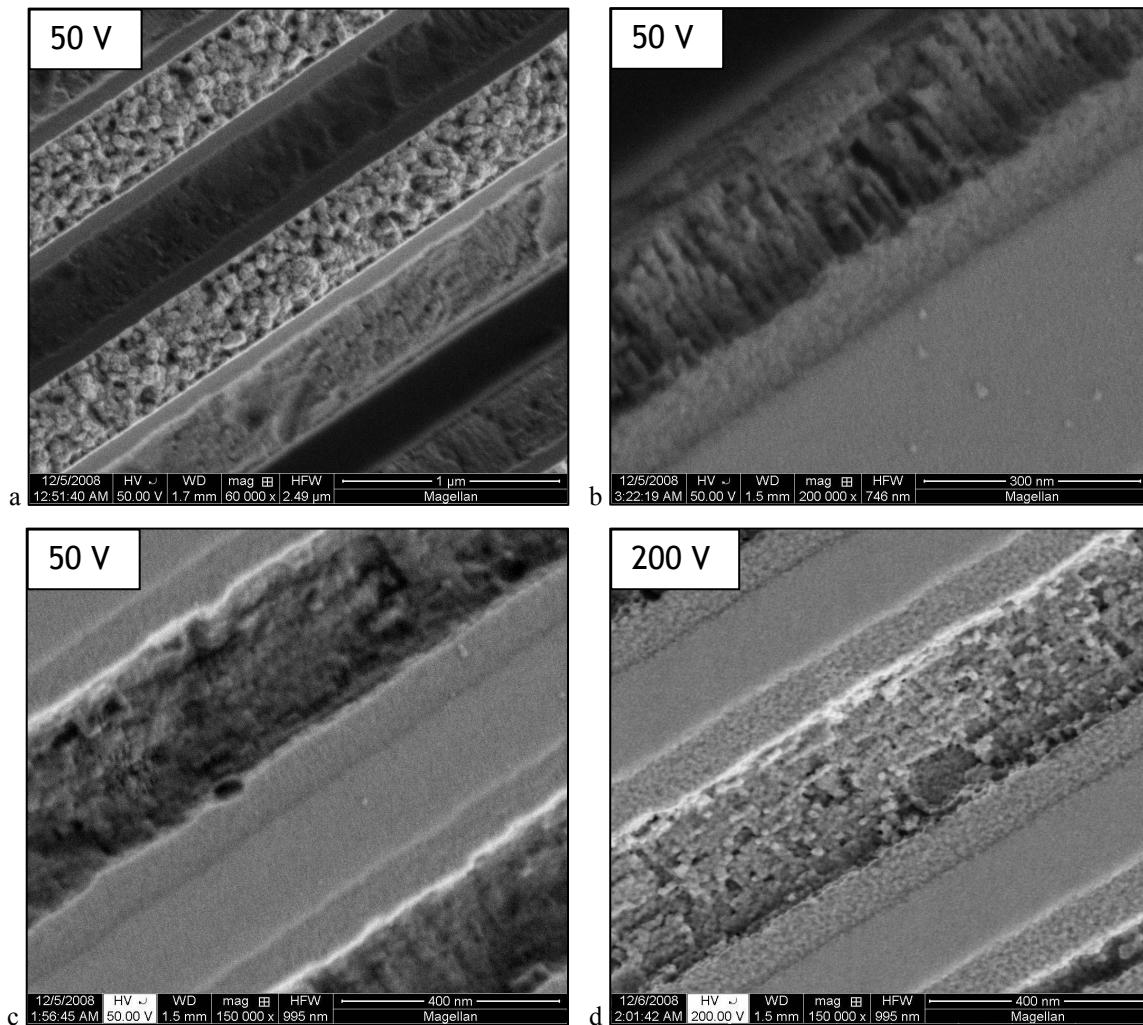


Fig. 3. Very low kV top-down characterization of the surface of a deprocessed integrated circuit using UC+BD and the TLD. The horizontal field width (HFW) is respectively (a) 2.49 μm, (b) 746 nm and (c), (d) 995 nm (Sample courtesy of ST Microelectronics Grenoble and Malta).

The characterization of the surface of a deprocessed integrated circuit at a beam landing voltage of 50 V is presented in figure 3. For all images, the UC mode is active, the sample set at 0° tilt and a working distance of 1.5 mm, and secondary electrons are collected by the TLD. For figures 3a-c a primary beam voltage of 1.05 kV is used, decelerated by $V_s = -1.0$ kV, whilst in 3d a beam voltage of 1.2 kV is used to give a landing voltage of 200 V. Rich topographic contrast and details can be seen at high and very high magnifications, especially from the areas of the sample that were chemically etched (fig. 3a and 3b). On the smooth surface of an unprocessed area (lower right side of fig. 3b), nanometer size particles are clearly resolved. Figure 3b also demonstrates the remarkable probe size obtained at very low beam landing energy by the Magellan, consistent with the outstanding 2.7 nm resolution at 50 V measured by Young et al [7] following the FEI edge resolution method [12]. As illustrated in figures 3c-d, moving the beam landing voltage from 200 V down to 50 V leads to a degradation of the resolution, consistent with the calculated theoretical probe size using BD+UC (respectively 0.8 nm and 1.7 nm at 200 V and 50 V beam landing voltage) [7], but more surface details are becoming visible (particles on the smooth surfaces). It is eventually worth noting that the samples in figures 2 and 3 were exposed to a mild surface cleaning (using the Magellan integrated plasma cleaner) and that the image acquisition was performed while keeping the liquid nitrogen-cooled cryo-cleaner active to minimize the adsorption of hydrocarbons. As a result, none of the images shot at 200 V or below display any visible trace of contamination.

3. HIGH RESOLUTION IN LOW-VOLTAGE STEM MODE

Any SEM with the ability to operate at a beam voltage of 10-30 kV can be turned into a low-voltage STEM (LV-STEM) system, or STEM-in-SEM, provided that the sample is thin enough for electrons to be transmitted and that a suitable detector can be placed under the sample. Here the term “low voltage STEM” is to distinguish from dedicated TEM/STEM systems, which typically resort to an 80-300 kV beam. The interest in low-voltage STEM started growing several years ago, as improved resolution and contrast mechanisms different from those of secondary or backscattered electrons could be obtained [13]. With respect to resolution, STEM-in-field-emission-SEM typically specifies below the nanometer level nowadays. Using some optics refinements, such as in the Hitachi S-5500 where the sample is located directly inside the objective lens, the observation of carbon lattice fringes was demonstrated [4]. While LV-STEM does not compete in resolution against dedicated S/TEMs, a sub-30 kV beam offers a greater scattering contrast especially in the case of low atomic number elements and low density materials, making it ideal for the characterization of polymers or biological samples [14]. Also, some materials may undergo structural modifications under a fixed TEM beam, while being successfully characterized by a LV-STEM method [15].

Like sub-1 kV SEM, LV-STEM deals with a minimized electron interaction volume (as the sample is very thin), hence resolution is improved, charging is dramatically reduced and less beam energy is transferred to the sample – resulting in less damage to the sample and barely noticeable contamination. Practically, both are also able to cover low and high magnifications. But while very low beam landing voltages focus primarily on highest surface sensitivity, LV-STEM offers greater possibilities for materials contrast, especially using recent solid-state multi-segment STEM detectors capable of separating bright field (BF), dark field (DF) and high angular annular dark field (HAADF) signals (see fig. 4). The bright field ring, on-axis with the electron beam, collects only weakly scattered transmitted electrons, while the dark field outer rings collect electrons scattered at higher angles, resulting in an image contrast associated with the atomic number and density of the elements in the sample.

3.1 Implementing LV-STEM in the XHR SEM

As the Magellan XHR SEM does not rely on an in-lens design, implementing a LV-STEM does not pose special difficulties. For the following work, the LV-STEM configuration illustrated in figure 4 is used. The Magellan XHR SEM is operated in high kV regimes (20-30 kV), with the UC mode off (chromatic aberrations are negligible at such high kVs). A 14-segment solid-state diode is inserted below the pole piece of the objective lens, and a thin sample placed between the two of them. The distance between the detector and the sample can be varied, for our experiments it is set to approximately 10 mm.

The different LV-STEM modes as performed in the Magellan XHR SEM are presented in figure 5, on a 56nm NAND memory device. The thin sample was prepared using a DualBeam focused ion beam (FIB) cutting, polishing and in-situ transfer to a TEM grid method. The material contrast between the polysilicon (i), silicide (ii) and ONO (oxide-nitride-oxide) layer (iii) is clearly enhanced when going to the dark field modes.

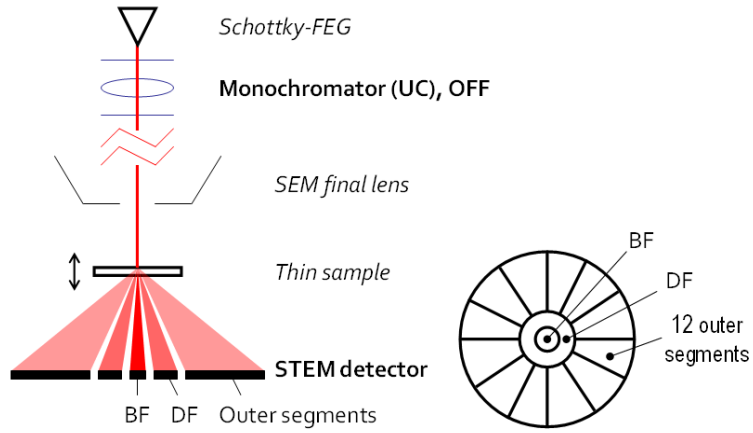


Fig. 4. LV-STEM configuration used in the XHR SEM

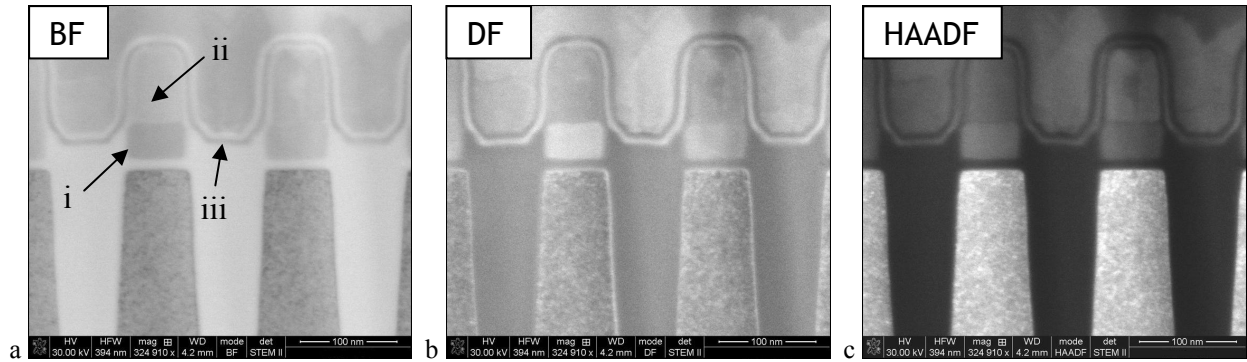


Fig. 5. 56nm NAND memory device imaged in XHR SEM LV-STEM (a) BF, (b) DF and (c) HAADF modes. Labeled regions are polysilicon (i), silicide (ii) and ONO layer (iii)

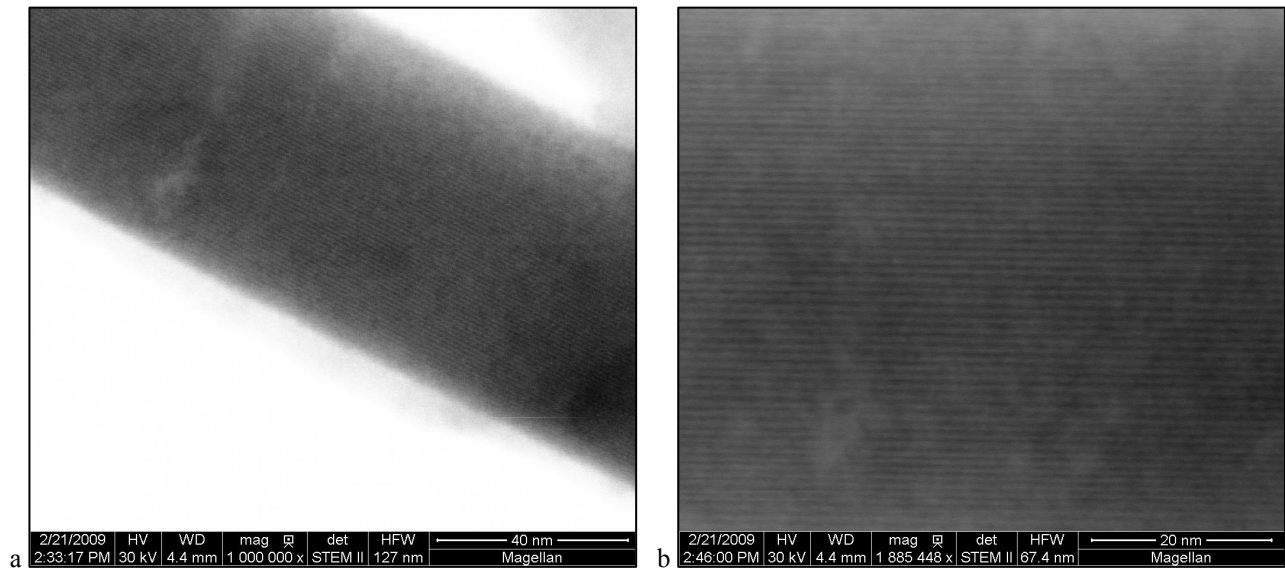


Fig. 6. XHR SEM BF LV-STEM images of a crocidolite asbestos sample.

3.2 XHR SEM LV-STEM on a Crocidolite Asbestos sample

To assess the LV-STEM performance of the Magellan XHR SEM, a crocidolite asbestos sample was chosen. Crocidolite fibers are finely textured and hair-like, and have gained their (un)popularity from causing lung cancers in those involved in the process of extracting (mining) them [16] and using them for industrial purposes such as thermally insulating materials or in cigarette components [17]. Crocidolite asbestos also turns out to be an established calibration specimen for S/TEM, displaying good diffraction patterns. Its (020) planes parallel with the long axis of the crystals are of the 0.903 nm spacing; the (021) planes of spacing 0.452 nm lie at about 60 degrees to this [18].

The bright field images of a crocidolite asbestos sample are presented in figure 6. The crystal lattice planes are nicely visible above 1Mx Polaroid magnification (figure 6a). From figure 6b, we measure an average plane spacing of 0.9 nm to 1.0 nm, indicating that the (020) plane is clearly resolved. These results give a good indication both of the flexibility provided by the high precision stage to position the sample in the right orientation, but also confirm the ability of the Magellan to resolve 0.9 nm crystal plane spaces in its LV-STEM mode. Further work is currently on-going with smaller plane spaces to assess the instrument resolution limit.

4. HIGH AND LOW BEAM VOLTAGE INFORMATION COMPLEMENTARITY

Both the XHR LV-SEM and LV-STEM modes can be applied to the same sample, in order to collect both surface and internal nanometer-scale data. This method was used for instance to characterize carbon nanotubes (CNT) activated with tin-palladium particles [19]. LV-STEM is of particular interest for the study of CNTs, as the beam energy used is well below the threshold where material alteration or damage would happen. An example of CNTs imaged in 30 kV LV-STEM and 200 V LV-SEM modes is presented in figure 7. LV-STEM was originally preferred over LV-SEM to characterize CNTs, because lower energies SEM characterization would risk causing a rapid growth of hydrocarbonaceous contamination, resulting for instance in inaccurate metrology when measuring the diameter of the CNT is at stake. Looking in particular at figure 7b, the contamination is again barely visible; LV-SEM can thus be effectively used to learn more from the surface of nanotubes.

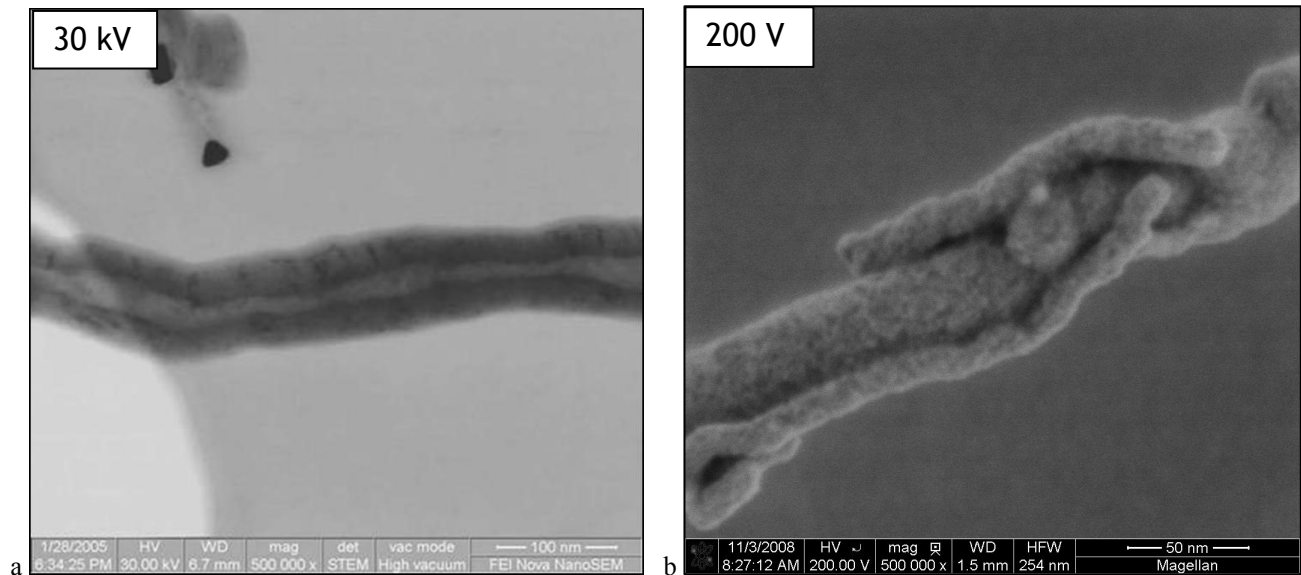


Fig. 7. Complementary information from CNTs: (a) internal structure, observed in BF mode using a 30kV electron beam with the field-emission SEM Nova NanoSEM and (b) surface information obtained with a 200V electron beam landing energy with the Magellan XHR SEM.

5. CONCLUSIONS

The XHR SEM demonstrates that extended characterization versatility can be maintained in a high resolution SEM, combining traditional characterization with LV-SEM and LV-STEM. With landing energies between 50 eV and 500 eV, very high surface sensitivity and spatial resolution are achieved, thanks to the dual operation of the monochromator and beam deceleration, as well as proper management of both sample and microscope chamber cleanliness. With the implementation of a multi-segment solid-state detector and holder for thin samples, high resolution in LV-STEM bright field, dark field and HAADF becomes possible, and sub-nanometer crystal plane spaces are revealed. Amongst the many other unexplored application opportunities, such as prototyping with a very small spot-size, low energy electron beam or analyzing using the large current capability of the Magellan, the XHR SEM LV-SEM and LV-STEM modes represent an exciting breakthrough to access unprecedented and complementary information from the same instrument.

ACKNOWLEDGEMENTS

The authors are grateful to FEI colleagues for many useful discussions and to the entire FEI Magellan development team. We also gratefully acknowledge the support of the Smart Mix Programme of the Netherlands Ministry of Economic Affairs and the Netherlands Ministry of Education, Culture and Science.

REFERENCES

- [1] Joy, D.C., "Scanning electron microscopy for materials characterization", *Current Opinion in Solid State and Materials Science* 2(4), 465-468 (1997).
- [2] Danilatos, G.D., "Foundation of environmental scanning electron microscopy", *Advances in Electronics and Electron Physics* 71, 109-250 (1988).
- [3] Kazumo, H., Honda, K., Matsuya, M., Date, M., Nielsen, C., "Field Emission SEM with a Spherical and Chromatic Aberration Corrector", *Proc. Microsc. Microanal.* 10(2), 1370-1371CD (2004).
- [4] Ngo, V.V., Hernandez, M., Roth, B., Joy, D.C., "STEM imaging of lattice fringes and beyond in a UHR in-lens field-emission SEM", *Microscopy Today* 15(2), 12-16 (2007).
- [5] Young, R.J., Templeton, T., Roussel, L.Y., Gestmann, I., Veen, G. van, Dingle, T., Henstra, S., "Extreme High Resolution SEM: a paradigm shift", *Microscopy Today* 16(4), 24-28 (2008).
- [6] Müllerová, I., Frank, L., "Very low energy microscopy in commercial SEMs", *Scanning* 15, 193-201 (1993).
- [7] Young, R.J., Henstra, S., Chmelik, J., Dingle, T., Mangnus, A., Veen, G. van, Gestmann, I., "XHR SEM: Enabling extreme high resolution scanning electron microscopy", *Proc SPIE*, to be published (2009).
- [8] Joy, D. C., Joy, C. S., "Low voltage scanning electron microscopy", *Micron* 27, 247-263 (1996).
- [9] Askary, F., Sullivan, N. T., "Redefining Critical in Critical Dimension Metrology", *Proc. SPIE* 4344, 815-826 (2001).
- [10] Müllerová, I., Frank, L., "Very low scanning electron microscopy", *Modern Research and Educational Topics in Microscopy*, 795-804 (2007).
- [11] Vldar, A. and Postek, M., "Electron Beam-Induced Sample Contamination in the SEM", *Proc. Microsc. Microanal.* 11(2), 764-765CD (2005).
- [12] Rieger, B., Veen, G. van, "Method to determine image sharpness and resolution in scanning electron microscopy images", *Proc. EMC '08* 1, 613-614 (2008).
- [13] Tracy, B., Alberi, K., "Adopting low-voltage STEM and automated sample prep to perform IC failure analysis", *MicroMagazine* July '04, 87-93 (2004).
- [14] Golla, U. et al, "Contrast in the transmission mode of a low-voltage scanning electron microscope", *J. Microscopy* 173(3), 219-225 (1994).
- [15] Russias, J., Frizon, F., Cau-Dit-Coumes, C., Malchere, A., Douillard T., Jousot-Dubien, C., "Incorporation of Aluminium into C-S-H structures: from synthesis to nanostructural characterization", *J. Am. Ceram. Soc.* 91(7), 2337-2342 (2008).
- [16] Musk, A.W., de Klerk, N.H., Reid, A., Ambrosini, G.L., Fritschi, L., Olsen, N.J., Merler, E., Hobbs M.S.T., Berry, G., "Mortality of former crocidolite (blue asbestos) miners and millers at Wittenoom", *Occupational and Environmental Medicine* 65, 541-543 (2008).

- [17] Longo, W.E., Rigler, M.W., Slade, J., “Crocidolite Asbestos Fibers in Smoke from Original Kent Cigarettes”, *Cancer Research* 55, 2232-2235 (1995).
- [18] PELCO® Technical Notes, Lattice Plane Resolution Tests, available at: [PELCO® Technical Notes, Lattice Plane Resolution Tests \(PDF 741kb\)](#)
- [19] Probst, C., Gauvin, R., Drew, R.A.L., “Imaging of carbon nanotubes with tin-palladium particles using STEM detector in a FE-SEM”, *Micron* 38, 402-408 (2007).

See Beyond at FEI.com

World Headquarters
Phone: +1.503.726.7500

FEI Europe
Phone: +31.40.23.56000

FEI Japan
Phone: +81.3.3740.0970

FEI Asia
Phone: +65.6272.0050

